WING DESIGN FOR A HIGH-SPEED CIVIL TRANSPORT USING A DESIGN OF EXPERIMENTS METHODOLOGY

Anthony A. Giunta*, Vladimir Balabanov*, Dan Haim†
Bernard Grossman‡, William H. Mason§, Layne T. Watson¶
Multidisciplinary Analysis and Design (MAD) Center for Advanced Vehicles
Virginia Polytechnic Institute and State University
Blacksburg, Virginia 24061-0203
and
Raphael T. Haftka#
Department of Aerospace Engineering, Mechanics and Engineering Science, University of Florida
Gainesville, Florida 32611-6250

Abstract

The presence of numerical noise inhibits gradient-based optimization and therefore limits the practicality of performing aircraft multidisciplinary design optimization (MDO). To address this issue, a procedure has been developed to create noise free algebraic models of subsonic and supersonic aerodynamic performance for use in the MDO of high-speed civil transport (HSCT) configurations. This procedure employs methods from statistical design of experiments theory to select a set of HSCT wing designs (fuselage/tail/engine geometry fixed) for which numerous detailed aerodynamic analyses are performed. Polynomial approximations (i.e., *response surface models*) are created from the aerodynamic data to provide analytical models relating aerodynamic quantities (e.g., wave drag and drag-due-to-lift) to the variables which define the HSCT wing configuration. A multidisciplinary design optimization of the HSCT is then performed using the response surface models in lieu of the traditional, local gradient based design methods. The use of response surface models makes possible the efficient and robust application of MDO to the design of an aircraft system. Results obtained from five variable and ten variable wing design problems presented here demonstrate the effectiveness of this response surface modeling method.

* Graduate Research Assistant, Dept. of Aerospace and Ocean Engineering, Student Member AIAA
† Graduate Research Assistant, Dept. of Computer Science
‡ Professor and Head, Dept. of Aerospace and Ocean Engineering, Associate Fellow AIAA
§ Professor of Aerospace and Ocean Engineering, Associate Fellow AIAA
¶ Professor of Computer Science and Mathematics
# Professor of Aerospace Engineering, Mechanics and Engineering Science, Associate Fellow AIAA

1. Introduction

Multidisciplinary design optimization (MDO) has received considerable attention in the aircraft industry as manufacturers employ concurrent engineering design practices in an attempt to reduce the time to market of new products. In these efforts, MDO practitioners would like to use the highest fidelity analysis methods as early as possible in the design process, preferably before the aircraft design is *frozen.* However, the realities of finite computational resources and time constraints limit the extent to which the high fidelity analysis methods may be applied early in the design process.

Computer models produce numerical noise as a result of the incomplete convergence of iterative processes, round-off errors, and the discrete representation of continuous physical phenomena (e.g., fluids) or objects (e.g., wing shapes). Such numerical noise is typically manifested as a high frequency, low amplitude variation in the results obtained from the computer models as design parameters vary. This oscillatory behavior creates numerous, artificial local optima and causes slow convergence or even convergence failures[1,2]. When a combined aerodynamic and structural analysis of an aircraft requires hours of CPU time on a supercomputer, numerous local optima and convergence difficulties are unacceptable for aircraft MDO.

To understand the link between numerical noise and computational expense in aircraft MDO, it is useful to consider the aerospace vehicle design process as traditionally divided into three phases: *conceptual, preliminary,* and *detailed.* Each of these design phases entails a particular of accuracy and computational expense. For example, in the conceptual level of design, each discipline (e.g., aerodynamics, structures, controls, or propulsion) is typically modeled using algebraic equations or simple numerical models which require only a few CPU seconds to compute. At the preliminary level of design, more computationally expensive numerical models are used, e.g., linear-theory aerodynamics or simple beam theory, which may require several CPU minutes. Similarly, at the detailed level of design more expensive methods such as Euler/Navier-Stokes aerodynamics and finite-element structural modeling are employed extensively. It is important to emphasize the computational expense of the detailed level methods in which several days and sometimes months of effort may be required to create the computational grid for a complete aircraft configuration and then tens of CPU hours are required on a supercomputer to evaluate the aerodynamic forces at a single altitude, Mach number, and angle-of-attack.

Traditional, derivative-based optimization methods[3] and derivative-free pattern search methods[4] require *hundreds* or *thousands* of aircraft evaluations to converge to an optimal design. Thus, while there are several computer programs which perform inexpensive, conceptual level aircraft MDO (e.g., ACSYNT[5], FLOPS[6]), preliminary level and detailed level aircraft *system* MDO in the presence of numerical noise remains computationally intractable.

Clearly, new strategies are needed to alleviate the optimization problems posed by numerical noise, and this has spurred much active research in both the aircraft design and numerical optimization communities[7,8]. These research efforts may be broadly divided into two categories: (1) novel modeling methods, and (2) novel optimization methods.

The novel modeling methods employ statistical techniques based on *design of experiments theory*[9] and *response surface modeling methodologies*[10]. Here, the aircraft designer performs a limited number of computational analyses or "numerical experiments" using experimental design theory to prescribe values for the independent variables. With the resulting data, the designer creates mathematical models using some type of function (e.g., polynomial functions, rational functions, interpolating functions, neural networks). The mathematical model is often called a *response surface model.* The designer then uses the response surface (RS) model in subsequent calculations during the optimization process. Response surface models filter out the numerical noise which inhibits derivative-based optimization. Although the computational expense of creating a response surface model may be significant, this cost is incurred prior to the use of the RS model in numerical optimization. Thus, a RS model may be evaluated hundreds or thousands of times during an optimization process without significant computational expense. There has been considerable interest in the application of RS modeling methods to MDO problems and examples of this research are given in References 11-18.

The novel optimization methods include a variety of both derivative-based and derivative-free techniques. The derivative-based methods include "collaborative optimization" schemes developed by Kroo[19] et al. in which the MDO problem is decomposed along disciplinary boundaries and a series of discipline-specific suboptimizations are performed under the authority of a system level optimizer. Another novel derivative-based method is the "implicit filtering" technique developed by Gillmore and Kelley[20] which employs a scheme where the step size used in finite-difference gradient estimates is systematically varied until convergence using several step sizes is attained. The novel derivative-free methods include pattern search schemes such as genetic algorithms[21] and simulated annealing[22,23], along with modern simplicial search algorithms[24].

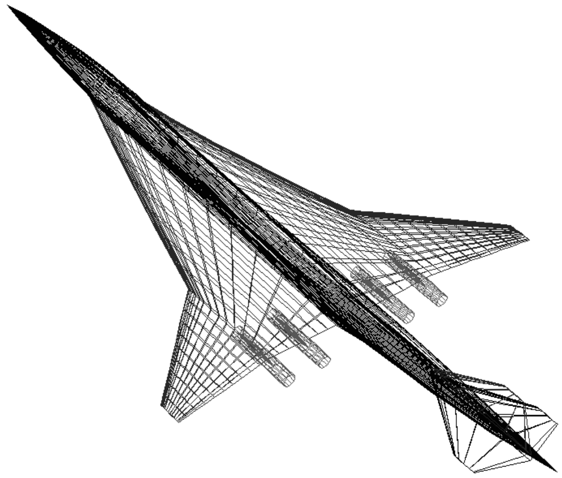

Figure 1. A typical HSCT configuration.

A method proposed here to overcome the difficulties poised by numerical noise in aircraft MDO is termed *variable complexity response surface modeling* (VCRSM). The multidisciplinary design optimization of a High-Speed Civil Transport (HSCT) aircraft (Figure 1) is used as a testbed for the VCRSM method. The design of an HSCT is an ideal MDO test case since the technical and economic feasibility of such an aircraft relies on synergistic interactions between the various aircraft design disciplines.

The *variable complexity* portion of VCRSM denotes the use of both conceptual level and preliminary level aircraft analysis methods. Here, the conceptual level methods are used to analyze numerous HSCT wing designs and to identify which of the wing designs merit further consideration. The preliminary level analysis methods are then used to evaluate some of the promising HSCT wing designs. The *response surface modeling* portion of VCRSM denotes the use of two statistical

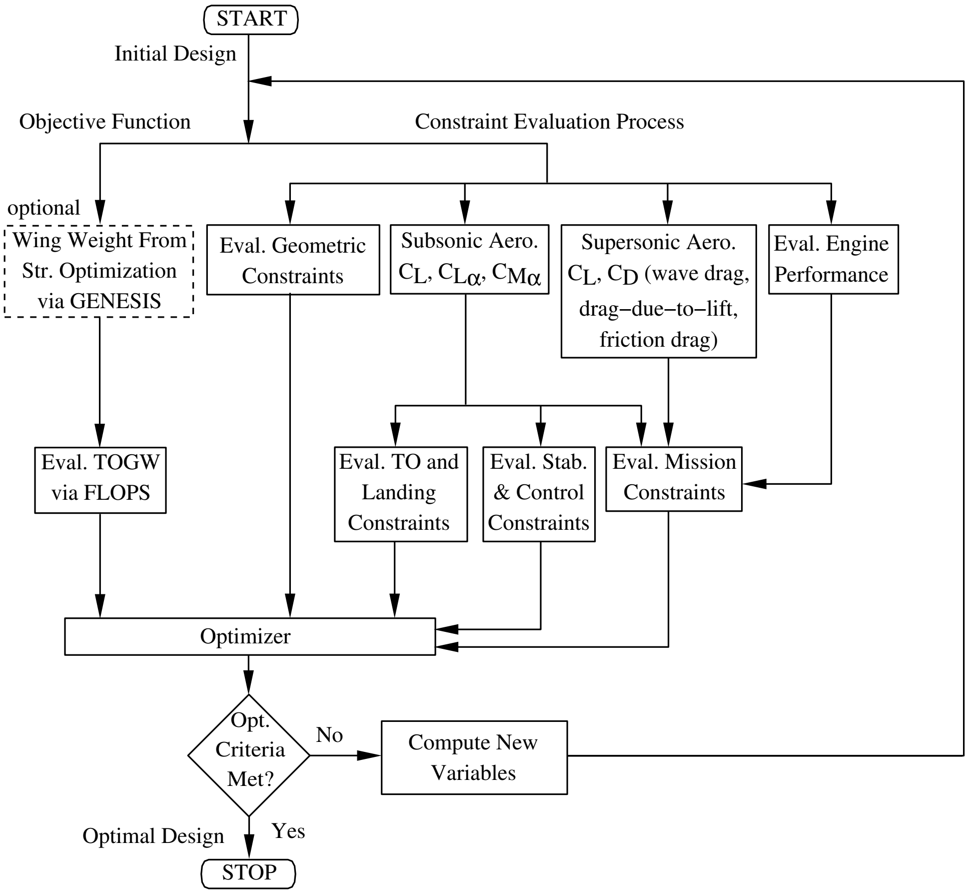

Figure 2. Multidisciplinary optimization method for HSCT design.

methods, design of experiments theory and response surface modeling. Here, design of experiments theory is used to select the HSCT wing designs which will be analyzed with the conceptual level and preliminary level analysis methods, and response surface models are created from the aerodynamic data resulting from the preliminary level analyses. The response surface models remove the numerical noise present in the preliminary level analyses and are computationally inexpensive to evaluate. The response surface models are then used for HSCT wing design optimization in lieu of the original, noise producing aerodynamic analysis methods.

For this study, response surface models are used to approximate four aerodynamic quantities as functions of the geometric variables which define the HSCT wing. These four aerodynamic quantities are supersonic volumetric wave drag, two components of supersonic drag-due-to-lift, and the subsonic lift curve slope. Two HSCT wing design cases, the first involving five variables and the second involving ten variables, were studied. In each case, the fuselage and tail layouts for the HSCT were held fixed while only the five or ten variables relating to the wing geometry were varied.

Although not discussed in this paper, parallel computing is crucial in reducing the computational expense of using the VCRSM method for aircraft MDO. See Reference 25 for details on how parallel computing strategies are employed in the VCRSM method.

The remainder of this paper is divided in the following manner. Section 2 contains a description of the HSCT configuration along with the analysis and optimization methods used in this study. This includes descriptions of the five and ten variable wing design problems. Section 3 reviews issues concerning numerical noise and the difficulties it introduces into optimization problems. Section 4 details the statistical techniques underlying the VCRSM method and Section 5 describes how the VCRSM method is used to perform aircraft MDO. Sections 6 and 7 contain the results from the five and ten variable HSCT wing design problems, and Section 8 concludes the paper.

2. HSCT Design Optimization

2.1 Design Tools

The design problem is to minimize the takeoff gross weight (TOGW) for a 250 passenger High-Speed Civil Transport with a range of 5,500 nautical miles and a cruise speed of Mach 2.4. For these efforts we have developed a suite of conceptual level and preliminary level analysis and design tools which include several software packages obtained from NASA along with in-house software. An abbreviated list of the HSCT analysis and design software is given in Table 1 and a description of these tools is given in Reference 2. The numerical optimization software is the commercially available program DOT[26] (Design Optimization Tools). DOT offers several algorithms for performing constrained optimization and we employ its sequential quadratic programming (SQP) optimization option. Figure 2 shows how the analysis and optimization tools are coupled to perform HSCT design optimization.

Currently, detailed level analysis tools (e.g., Euler or Navier-Stokes aerodynamic analyses) are not included because of their high computational expense. However, we have been evaluating an Euler/Navier-Stokes solver for use in HSCT design. These efforts are detailed in Reference 27.

Table 1. Analysis and optimization tools for HSCT design.

Method	**Description**
Subsonic Aero.	In-house Codes
Supersonic Aero.	In-house Codes
	WINGDES[28] (NASA)
	Harris Wave Drag Code[29] (NASA)
Propulsion	In-house Codes
Stability & Control	In-house Codes
TO/Landing Performance	In-house Codes
Mission Performance	In-house Codes
Weights and Structures	FLOPS[6] (NASA)
	GENESIS[30] (VMA, Inc.)
Optimizer	DOT[26] (VR&D, Inc.)

2.2 HSCT Parametrization

The HSCT configuration and mission are defined using 29 variables (Appendix, Table A-1). Twenty-six of these variables describe the geometric layout of the HSCT and three variables describe the mission profile. The airfoil and planform variables are shown in Figure 3. In this parametrization, eight variables describe the wing planform, eight variables define the area ruled fuselage shape distribution, five variables define the wing leading edge and airfoil section properties, two variables define the engine nacelle locations, two variables define the horizontal and vertical tail areas, and one variable defines engine thrust. For this HSCT design problem the fuselage has a fixed length of 300 ft and an internal volume of 23,720 ft^3.

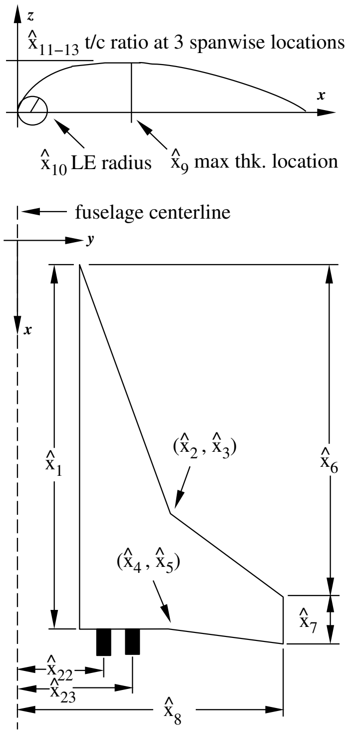

Figure 3. HSCT wing variables for the 29 variable optimization problem.

The idealized mission profile is divided into three segments: takeoff, supersonic cruise/climb at Mach 2.4, and landing. The three mission design variables are fuel weight, starting altitude for the supersonic cruise/climb segment, and rate-of-climb during the supersonic cruise/climb segment. If the HSCT reaches the maximum ceiling of 70,000 ft, supersonic cruise at Mach 2.4 is maintained at that altitude for the duration of the supersonic mission leg.

The HSCT design employs 69 nonlinear inequality constraints which consist of both geometric constraints (e.g., all wing chords $\geq 7.0ft$), and aerodynamic/performance constraints (e.g., C_L at landing $\leq$ 1, and range $\geq$ 5,500 $naut.mi.$). These are listed in the Appendix in Table A-2. The HSCT design objective is to minimize TOGW, where TOGW is a nonlinear, implicit function of the 29 design variables. In formal optimization terms this problem may be expressed as

$$\begin{aligned} &\min_{\hat{x} \in R^{29}} TOGW(\hat{x}) \\ &\text{subject to } g_i(\hat{x}) \leq 0, \qquad i = 1, \ldots, 69, \end{aligned} \tag{1}$$

where $\hat{x}$ is the 29-dimensional vector of design variables, and $g(\hat{x})$ is the 69-dimensional vector of nonlinear inequality constraints.

2.3 HSCT Wing Design - Five Variables

A simple five variable HSCT wing design problem is used to develop and validate the variable complexity response surface modeling method. This five variable problem is based on the 29 variable HSCT MDO problem described above. The five variables are wing root chord (C_{root}), wing tip chord (C_{tip}), thickness-to-chord ratio ($t/c\ ratio$), inboard leading edge sweep angle (Λ_{LE_I}), and fuel weight (W_{fuel}). Their initial values along with the minimum and maximum values are listed in Table 2.

Table 2. Five HSCT wing variables and initial values.

Variable	**Initial**	**Min.**	**Max.**
C_{root}	185.0 ft	148.0 ft	222.0 ft
C_{tip}	10.0 ft	8.0 ft	12.0 ft
Λ_{LE_I}	75.0°	68.3°	81.8°
$t/c\ ratio$	2.0%	1.6%	2.4%
W_{fuel}	315,000 lb	305,550 lb	324,450 lb

The wing planform and airfoil section definitions are shown in Figure 4. To uniquely define the wing planform, the length of the leading edge from the wing/fuselage intersection to the leading edge break is held constant at 150.0 ft, and the outboard leading edge sweep angle is held constant at 44.2°. For the airfoil section definitions, the chordwise location of maximum thickness is constant at 40.0 percent and the leading edge radius is constant at a value of 1/3 that of a NACA 6-series airfoil (i.e., the leading edge radius parameter is constant at a value of 2.63). Additionally, the vertical tail area is fixed at 700 ft^2, and the thrust is constant at 39,000 lb per engine. A horizontal tail is not considered for this aircraft. The mission profile also is simplified from the 29 variable HSCT design problem to include only a supersonic cruise leg and landing. The altitude for the Mach 2.4 supersonic cruise mission is constant at 65,000 ft. Landing constraints on both the overall lift coefficient and 18 wing section lift coefficients are examined for emergency landing situations. For the five variable design problem there are 42 constraints (Appendix, Table A-3) and the optimization problem may be expressed as

$$\begin{aligned} &\min_{\hat{x} \in R^5} TOGW(\hat{x}) \\ &\text{subject to } g_i(\hat{x}) \leq 0, \qquad i = 1, \ldots, 42, \end{aligned} \tag{2}$$

where $\hat{x}$ is the five-dimensional vector of design variables, and g is the 42-dimensional vector of nonlinear inequality constraints.

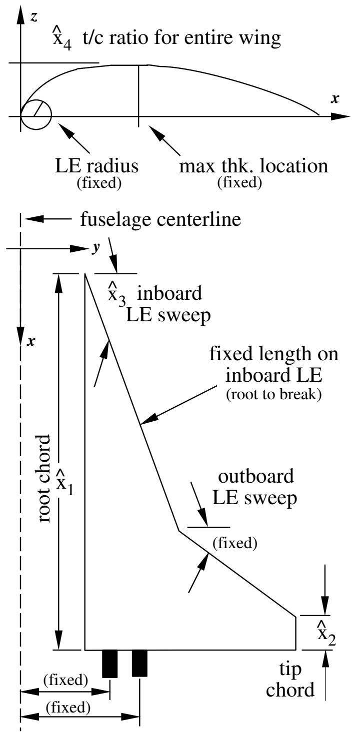

Figure 4. HSCT planform for the five variable optimization problem.

2.4 HSCT Wing Design - Ten Variables

A ten variable HSCT wing design problem was examined to further validate the VCRSM method. The ten variables for this design problem are wing root chord (C_{root}), wing tip chord (C_{tip}), wing semi-span (b_{half}), inboard leading edge sweep angle (Λ_{LE_I}), outboard leading edge sweep angle (Λ_{LE_O}), chordwise location of maximum thickness ($max.\ thk.$), leading edge radius parameter ($R_{LE}\ param.$), thickness-to-chord ratio ($t/c\ ratio$), spanwise location of the inboard nacelle ($b_{nacelle}$), and fuel weight (W_{fuel}). Their initial values along with the minimum and maximum values are listed in Table 3. Figure 5 shows the airfoil and planform variables for this problem.

As in the five variable problem, the area-ruled fuselage shape is held constant, the length of the leading edge from the wing/fuselage intersection to the leading edge break is held constant at 150.0 ft, the vertical tail area is fixed at 700 ft^2, and the thrust is held constant at 39,000 lb per engine. Additionally, the outboard nacelle is fixed at a spanwise distance of 6 ft from the centerline of the inboard nacelle and the Mach 2.4 cruise altitude is constant at 70,000 ft.

Table 3. Ten HSCT wing variables and initial values.

Variable	Initial	Min.	Max.
C_{root}	174.0 ft	139.2 ft	208.7 ft
C_{tip}	8.1 ft	6.5 ft	9.7 ft
b_{half}	73.9 ft	66.5 ft	81.3 ft
Λ_{LE_I}	71.9°	65.4°	78.3°
Λ_{LE_O}	44.2°	40.2°	48.2°
max. thk.	39.6%	31.7%	47.5%
R_{LE} *param.*	2.6	2.1	3.2
t/c ratio	2.3%	1.8%	2.7%
$b_{nacelle}$	20.9 ft	16.7 ft	25.1 ft
W_{fuel}	310,000 lb	300,700 lb	319,300 lb

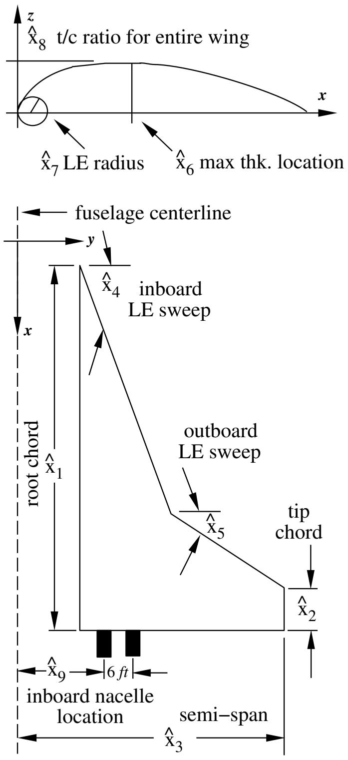

Figure 5. HSCT planform for the ten variable optimization problem.

Along with the 42 constraints from the five variable wing design problem, there are seven additional constraints on the subsonic aerodynamic performance at landing. The first of these is an angle-of-attack (AOA) constraint of AOA $\leq 13°$ at landing. The other six are runway strike constraints on the wing tip and engines at the landing AOA with both 0° and 5° roll angles. The ten variable HSCT wing design optimization problem may be expressed as

$$\begin{aligned} &\min_{\hat{x} \in R^{10}} TOGW(\hat{x}) \\ &\text{subject to } g_i(\hat{x}) \leq 0, \qquad i = 1, \ldots, 49, \end{aligned} \tag{3}$$

where $\hat{x}$ is the ten-dimensional vector of design variables, and g is the 49-dimensional vector of nonlinear inequality constraints.

3. Numerical Noise Issues

3.1 Noise Sources

Convergence difficulties were encountered in previous research on the aerodynamic-structural optimization of the HSCT[1,2]. The convergence problems were traced to *numerical noise* in the computation of aerodynamic lift and drag components. This oscillatory behavior creates numerous, artificial local optima and leads to convergence failures or slow convergence to poor designs.

The lift and drag values predicted by some of the aerodynamic analysis tools are sensitive to slight changes in the aircraft design. This sensitivity is illustrated in Figure 6 which shows supersonic volumetric wave drag (C_{Dwave}) calculated for an HSCT cruising at Mach 2.4. Here, the analysis method uses the Harris wave drag code[29] where all of the HSCT design variables are fixed, with the exception of the wing semi-span which is varied from 50 to 100 ft. As the semi-span increases, numerical noise is created by a high frequency variation in the calculated wave drag values. Physically, wave drag should change smoothly as the wing shape is varied. Note that this numerical noise occurs on an extremely small scale with variations in wave drag on the order of 0.02 to 0.1 drag counts (drag in counts = $C_D \times 10^4$). The Harris wave drag code has an accuracy of approximately 0.5 to 1.0 drag counts and was not developed with optimization in mind. Hence, wave drag variations of 0.02 to 0.1 counts were considered inconsequential by the original programmers.

Figure 6 also shows a quadratic response surface model obtained by performing a least squares curve fit to the noisy data. The RS model smoothes out the various scales of numerical noise present in the data while it captures the global trends of the variation in wave drag.

The problems associated with numerical noise in optimization are ubiquitous in engineering, with examples appearing in the structural optimization software[31] used in HSCT aerodynamic-structural design research related to this study, and in an Euler flow solver used for a nozzle design study[32].

Derivative-based optimization methods employ analytic or finite difference derivatives of the objective function and constraints with respect to the design variables. Finite differences naively applied to noisy function values can produce grossly erroneous derivative estimates, which may lead to slow or incomplete convergence. Often the result is that the optimizer identifies many locally optimal designs, each of which is obtained by starting the optimization process from a different initial design. Here, the optimization process is deterministic, i.e., the same optimal design is found for a specific set of initial variables. However, numerical noise creates artificial local optima which trap the optimizer far from the true optimal design. Gillmore and Kelley[20] have developed derivative-based optimization methods in which the finite difference step size is systematically varied until convergence is attained. This method has been successful on a number of problems in which numerical noise has posed optimization difficulties.

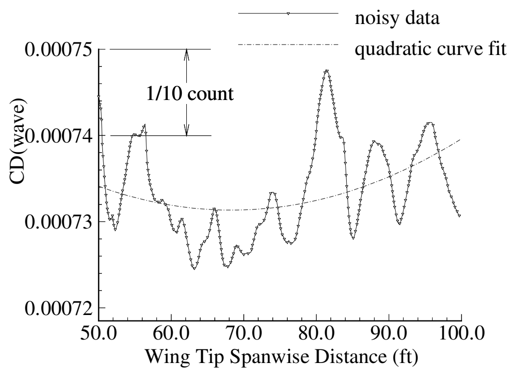

Figure 6. Numerical noise in computed wave drag.

3.2 Smooth Response Surface Models

The VCRSM method counters the adverse affects of numerical noise by creating smooth, polynomial models to replace the noise producing aerodynamic analysis codes used in this study. This is accomplished by analyzing many different HSCT configurations prior to starting the design optimization. Smooth polynomial models (i.e., response surface models) are then created by fitting curves to the noisy aerodynamic analysis data. The aerodynamic analysis tools which create numerical noise are then replaced by the smooth response surface models and the design optimization is performed. Without numerical noise to inhibit optimization, there is a greater probability that the globally optimal design will be found, regardless of the initial variable values used to start the optimization.

In addition to the C_{Dwave} analyses, two components of the supersonic drag-due-to-lift (C_{Dlift}) are affected by numerical noise as well. Here, supersonic drag-due-to-lift is calculated as

$$C_{Dlift} = (\frac{1}{C_{L\alpha}} - k_t \frac{C_T}{{C_L}^2}){C_L}^2, \tag{4}$$

where $C_{L\alpha}$ is the supersonic lift curve slope at M=2.4, $C_T/{C_L}^2$ is the leading edge thrust term, and k_t is an attainable leading edge thrust factor. The numerical noise in the drag-due-to-lift evaluation occurs in the supersonic lift curve slope and leading edge thrust terms. The "Mach-box" methods of Carlson[28] et al. utilize a wing discretization scheme that is sensitive to planform changes. Thus, slight modifications to the leading and trailing edge sweep angles, along with changes in the location where the Mach angle intersects the leading edge, produce noisy variations in the predicted drag. As was the case for the noise levels in the wave drag analyses, the numerical noise in the drag-due-to-lift calculations is within the intended accuracy of the analysis method.

In addition to improving optimization convergence and reliability, the response surface models have the added benefit of being extremely inexpensive to evaluate during optimization. This is of paramount importance since a particular aerodynamic analysis may be needed thousands of times during the optimization process. Thus, it becomes advantageous to also use response surface models to approximate the results obtained from expensive analysis methods, even though the expensive analysis tools may not produce numerical noise. In this manner, the computational expense is incurred in the creation of the response surface model and the resulting cost for use of the model during optimization is computationally insignificant. One such relatively expensive analysis method is a vortex-lattice method which is used to estimate subsonic aerodynamic performance. In particular, the subsonic lift curve slope $C_{L\alpha}$ at M=0.2 is the parameter of interest.

In the five variable HSCT wing design problem, RS models for $C_{Dwave}, C_{L\alpha}$ at M=2.4, and $C_T/{C_L}^2$ are used to approximate supersonic aerodynamic performance. Note that subsonic aerodynamic performance is not considered for the five variable problem. The ten variable wing design problem employs the three supersonic RS models along with a RS model for $C_{L\alpha}$ at M=0.2 to estimate subsonic aerodynamic performance.

4. Statistical Methods

Experimental design theory[9] is a branch of statistics which provides the researcher with numerous methods for selecting the independent variable values at which a limited number of experiments will be conducted. The various experimental design methods create certain combinations of numerical experiments (analyses) in which the independent variables are prescribed at specific values or *levels.* The results of these planned experiments are used to investigate the sensitivity of some dependent quantity, identified as the *response,* to the independent variables. Other statistical techniques known as regression analysis and analysis of variance (ANOVA) are employed in the response sensitivity investigation. They are used to perform a systematic decomposition of the variability in the observed response values and to assign portions of the variability to either the effect of an independent variable or to experimental error. In using ANOVA with numerical experiments, numerical noise takes the place of experimental error.

4.1 Response Surface Modeling

A response surface methodology (RSM) is a formal process combining elements of experimental design, regression analysis, and ANOVA[10]. RSM employs these statistical methods to create functions, typically polynomials, to model the response or outcome of a numerical experiment in terms of several independent variables, e.g., wave drag expressed as a function of several wing planform variables.

In many RSM applications, either linear or quadratic polynomials are assumed to accurately model the selected response. Although this is certainly not true for all cases, RSM becomes prohibitively expensive when cubic and higher-order polynomials are chosen for experiments involving several variables. Giunta[1] et al. concluded that quadratic polynomial models were sufficiently accurate for HSCT configuration design.

A quadratic response surface model has the form

$$y = c_o + \sum_{1 \le j \le m} c_j x_j + \sum_{1 \le j \le k \le m} c_{jk} x_j x_k, \tag{5}$$

where y is the response, x_j represents the m design variables, and c_o, c_j, and c_{jk} are the unknown polynomial coefficients. Note that there are $n = (m+1)(m+2)/2$ coefficients in this quadratic polynomial. To estimate the unknown polynomial coefficients in the RS model, at least p response values must be available, where $p \geq n$. Under such conditions, the estimation problem may be formulated in matrix notation as $Y \approx \mathbf{X}c$, where Y is the p by 1 vector of observed response values, $\mathbf{X}$ is a p by n matrix of constants assumed to have rank n, and c is the n by 1 vector of unknown coefficients to be estimated. The least squares solution to $Y \approx \mathbf{X}c$ is $\hat{c} = (\mathbf{X}^T\mathbf{X})^{-1}\mathbf{X}^T Y$. Typically values for p of at least $1.5n$ to $2.5n$ are required to produce response surface models which accurately model the trends in the calculated data[1].

Besides the polynomial coefficients, the regression analysis also provides a measure of the uncertainty in these coefficients, called the t-statistic. The reciprocal of the t-statistic is an estimate of the standard deviation of each coefficient as a fraction of its value. Accordingly, coefficients with "low" values for the t-statistic are not accurately estimated. It is the prerogative of the user to select the minimum allowable t-statistic. This choice typically depends on the number of numerical experiments (*degrees of freedom* (DOF) in the statistical lexicon) used to create the response surface model. For a coefficient estimated with at least of one degree of freedom, a 90 percent confidence interval requires a t-statistic of greater than 6.31 for that coefficient to be accurately estimated. This criterion will be used in all subsequent regression analyses.

Various procedures exist for removing coefficients with low t-statistics because leaving these coefficients in the response surface model may reduce the prediction accuracy of the model. A common measure of the utility of removing coefficients for improving the accuracy of the response surface is called the adjusted R^2 value ($R^2{}_{adj}$). The adjusted R^2 value is calculated as

$$R^2{}_{adj} = 1 - \frac{SSE/DOF_{SSE}}{SYY/DOF_{SYY}}, \tag{6}$$

where SSE (error sum of squares), SYY (total sum of squares), DOF_{SSE}, and DOF_{SYY} are obtained from ANOVA calculations[10]. If removing coefficients from the response surface model leads to substantial increases in $R^2{}_{adj}$, then it is recommended to remove them. The best possible value for $R^2{}_{adj}$ is 1.0.

4.2 Experimental Design Methods

4.2.1 Full Factorial Design

Prior to experimental design, the allowable range of each of the m variables is defined by lower and upper bounds. The allowable range is then discretized at equally-spaced levels. For numerical stability and for ease of notation the range of each variable is scaled to span $(-1, 1)$[10]. The region enclosed by the lower and upper bounds on the variables is termed the *design space,* the vertices of which determine an $m-$dimensional cube or *hypercube.* If each of the variables is specified at only the lower and upper bounds (two levels), the experimental design is called a 2^m full factorial. Similarly, a 3^m full factorial design is created by specifying the lower bound, midpoint, and upper bound (three levels) for each of the m variables. A 3^3 full factorial design is shown in Figure 7.

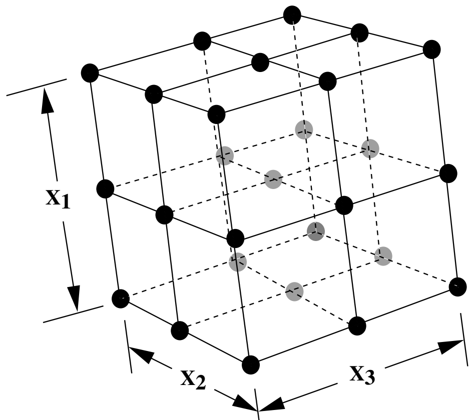

Figure 7. A 3^3 full factorial design (27 points).

The construction of a quadratic response surface model in m variables requires at least $n = (m+1)(m+2)/2$ response evaluations. A 3^m full factorial design provides ample response evaluations to permit the estimation of the RS model coefficients. For example, fitting a quadratic response surface model in three variables ($m = 3$) requires at least ten evaluations, and a 3^3 full factorial design provides 27 evaluations. However, as m becomes large the evaluation of both 2^m and 3^m full factorial designs becomes impractical (e.g., 2^{10} =1,024 and 3^{10} =59,049). A full factorial design typically is used for ten or fewer variables.

4.2.2 D-Optimal Design

RSM typically employs a full factorial or similar experimental design. However, full factorial designs are intended for use with rectangular design spaces and not the irregularly shaped (even nonconvex) design spaces that may arise in the HSCT design problems considered here. Previous studies[1,12,14] found that the D-optimality criterion[10,33] provides a rational means for creating experimental designs inside an irregularly shaped design space.

The objective of the D-optimality criterion is to select the set of p locations in a design space from a pool of q candidate locations ($q \geq p$), such that the quantity $|\mathbf{X}^T\mathbf{X}|$ is maximized. Note that the pool of q candidate locations is defined *a priori* by the user, and the p locations which maximize $|\mathbf{X}^T\mathbf{X}|$ are found iteratively using a numerical optimization method.

The set of p locations for which $|\mathbf{X}^T\mathbf{X}|$ is maximum is called a D-optimal experimental design. The statistical reasoning behind the creation of a D-optimal design is that it leads to response surface models for which the maximum variance of the predicted responses is minimized. In non-statistical terms, the D-optimality criterion ensures that the p locations are selected at points in the design space which will minimize the error in the estimated coefficients, $\hat{c}$, in the response surface model.

For this study, two methods were used to create D-optimal experimental designs. In the five variable problem, the commercial statistical package JMP[34] was used. JMP employs the "k-exchange" method of Mitchell[35] to select a set of p D-optimal locations from a user supplied list of q candidate locations. For the ten variable problem, JMP became computationally inefficient. Therefore, we programmed our own "k-exchange" method to efficiently create D-optimal experimental designs. Earlier work[1,14,25,31] used genetic algorithms to create D-optimal experimental designs.

5. The VCRSM Method

The construction of the response surface models may be viewed as a series of steps to be completed before the aircraft system optimization is performed. This methodology is illustrated in the flowchart shown in Figure 8.

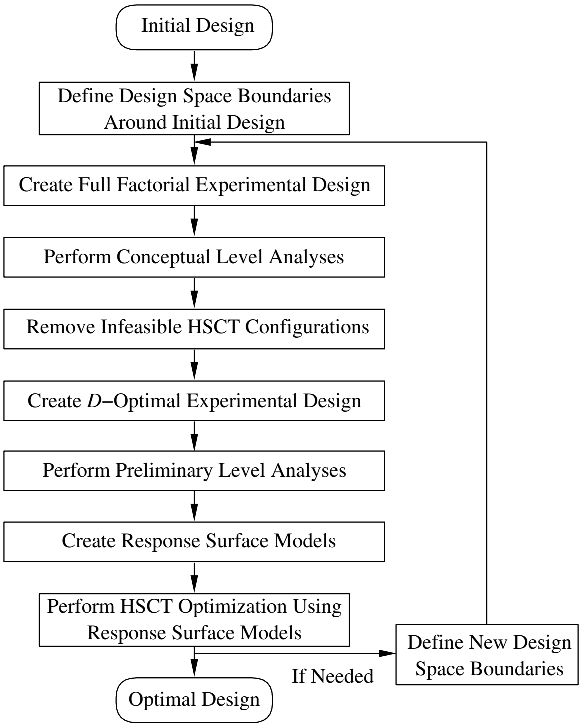

Figure 8. Flowchart depicting the use of the VCRSM method in HSCT design optimization.

Starting from an initial HSCT configuration, a 3^m or similar full factorial design is constructed with the initial HSCT at the center of the design space. The full factorial design points are evaluated using the computationally inexpensive conceptual level analysis tools, and the HSCT analyses are screened to eliminate any grossly infeasible HSCT configurations from consideration. Next, the D-optimality criterion is applied to select a subset of the remaining HSCT configurations for evaluation using the preliminary level analysis tools. Response surface models for the aerodynamic quantities are then constructed using the preliminary level analysis data. In the final step of the VCRSM method the response surface models are used in the HSCT optimization software to replace the noise producing aerodynamic analysis methods. Thus, optimization is conducted without the problems associated with numerical noise.

6. HSCT Wing Design - Five Variables

6.1 Conceptual Level HSCT Analyses

A 5^5 full factorial design (i.e., five levels in each variable) based on DOE methods was constructed around an initial HSCT configuration. The 3,125 (5^5) full factorial HSCT configurations were analyzed using the inexpensive conceptual level analysis tools. These 3,125

HSCT configurations were then screened to eliminate from consideration any grossly infeasible designs, i.e., those which exceeded any of the geometric constraints by more that five percent or any of the aerodynamic constraints by ten percent. After screening, 1,860 HSCT configurations remained.

6.2 Preliminary Level HSCT Analyses

In the next step of the VCRSM process, JMP was used to create a *D*-optimal experimental design comprised of 50 HSCT configurations out of the 1,860 remaining HSCT candidates. Note that at least 21 HSCT configuration analyses are needed to fit a quadratic polynomial in five variables. Choosing 50 HSCT configurations for analysis provides slightly more than double the minimum number of analyses. As described above, past research indicates that at least 1.5 to 2.5 times the minimum number of analyses are required. The distribution of the 50 *D*-optimal HSCT configurations within the design space yields a condition number of 18 for the matrix $\mathbf{X}$ in the least squares fit which creates the RS model. This indicates that the *D*-optimal HSCT configurations are positioned throughout the design space in a manner that allows accurate estimation of the RS model terms without significant numerical error.

Once selected, the 50 *D*-optimal HSCT configurations were evaluated using the preliminary level analysis methods and RS models were constructed from the analysis data for C_{Dwave}, $C_{L\alpha}$ (M=2.4), and $C_T/{C_L}^2$. Adjusted R^2 values were calculated as 0.9953, 0.9965, and 0.9908 for C_{Dwave}, $C_{L\alpha}$ (M=2.4), and $C_T/{C_L}^2$, respectively.

Of the 21 coefficients in the C_{Dwave} RS model, 15 had a *t*-statistic above 6.31. All linear terms were significant as were the quadratic terms for $C_{root}, t/c\ ratio$, and Λ_{LE_I}. The regression analysis procedure in JMP was then used to remove the less significant coefficients from the RS model and ${R^2}_{adj}$ was recomputed. However, ${R^2}_{adj}$ changed only from 0.9953 to 0.9956. Therefore, the complete (21 coefficient) polynomial RS model for C_{Dwave} was retained.

Regression analyses also were performed on the $C_{L\alpha}$ (M=2.4) and $C_T/{C_L}^2$ RS models. For the $C_{L\alpha}$ (M=2.4) model, 11 of the coefficients had *t*-statistic values greater than 6.31. The retained coefficients included all linear terms except for W_{fuel}, and quadratic terms for C_{root} and Λ_{LE_I}. Again, the recomputed ${R^2}_{adj}$ value changed only slightly from 0.9965 to 0.9969 so the complete RS model for $C_{L\alpha}$ (M=2.4) was used. For the $C_T/{C_L}^2$ model only seven coefficients were retained which included the linear terms C_{root}, C_{tip}, and Λ_{LE_I}, and the quadratic terms for C_{root} and Λ_{LE_I}. The recomputed ${R^2}_{adj}$ value improved only slightly from 0.9908 to 0.9913 so the complete RS model also was retained for $C_T/{C_L}^2$.

Another quantitative measure of the quality of the RS model is to evaluate the residual error in the least squares fit which creates the RS model. The residual error is the difference between the calculated response from the numerical experiment data and the predicted response from the RS model. The residual error is a composite measure of error due to numerical noise and error due to bias. Bias error occurs when using a low order polynomial RS model when the data have higher order trends. For the five variable HSCT optimization problem, the average error, root-mean-square (RMS) error, and maximum error are shown in Table 4, where the residual error calculations are performed for the data from the 50 HSCT analyses used to create the RS models. Here, the errors are expressed as a percentage of the total variation in each RS model. The small magnitude of the errors further indicates that the quadratic polynomials are good models of the data trends.

Table 4. Accuracy of the response surface models for the five variable HSCT optimization.

	Avg. Error	**RMS Error**	**Max. Error**
C_{Dwave}	0.82%	1.06%	3.07%
$C_{L\alpha}$ at M=2.4	0.24%	0.31%	0.88%
$C_T/{C_L}^2$	2.02%	2.46%	5.78%

The quality of the RS models is further shown by comparing the mission range of the initial HSCT computed using both the RS models and the original aerodynamic analysis methods. The range computed using the RS models is 5,579.7 *naut.mi.* whereas the range computed using the original methods is 5,509.7 *naut.mi.*, a difference of 1.27 percent.

6.3 HSCT Optimization - Five Variables

Figures 9 and 10 show optimization results for the five variable HSCT wing designs obtained with and without using the VCRSM method. As shown in Figure 9, there were slight changes in the planform geometry between the initial and optimal designs. Specifically, the initial and final designs are listed in Table 5. These design changes result in a savings of approximately 7,000 *lb* in the structural weight of the wing and about 10,000 *lb* of fuel weight. These weight savings more than offset the slight decrease in aerodynamic efficiency in the optimal wing which had a maximum lift-to-drag ratio $(L/D)_{max}$ of 9.76 compared to $(L/D)_{max}$ of 9.85 for the initial wing.

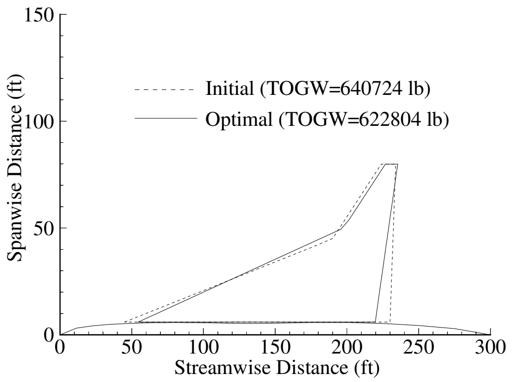

Figure 9. Five variable initial and optimal designs obtained using RS models.

For the optimal HSCT wing configuration, the range computed using the RS models is 5,499.2 *naut.mi.* whereas the range computed using the original methods is 5,443.2 *naut.mi.*, a difference of 1.03 percent. Since the true range is below 5,500 *naut.mi.*, the HSCT configuration would need to carry additional fuel to meet the range constraint. This would add approximately 5,000 *lb* to the TOGW of the HSCT, an increase of 0.80 percent in TOGW for the optimal HSCT configuration.

Table 5. Five HSCT wing initial and optimal variables.

Variable	Initial	Optimal
C_{root}	185.0 ft	165.2 ft
C_{tip}	10.0 ft	8.6 ft
Λ_{LE_I}	75.0°	72.9°
t/c $ratio$	2.0 %	2.2 %
W_{fuel}	315,000 lb	305,550 lb

In contrast, Figure 10 shows almost no change between the initial and optimal wing designs when the RS models were not used. This occurred because numerical noise in the wave drag and drag-due-to-lift calculations led to numerical noise in the TOGW and constraint calculations. This numerical noise created local minima in the design space which prevented the optimizer from locating the globally optimal wing design. The consequence of not using the RS models was a 14,000 *lb* difference in TOGW between the globally optimal design and the locally optimal design.

Similar results were obtained when different initial values for the variables were used in the HSCT optimization. With the RS models, the optimizer converged to the same globally optimal wing configuration. Without the RS models, the optimizer became trapped in different, artificial locally optimal wing configurations. The locally optimal wings yielded significantly higher values of TOGW than the optimal wing, often with considerably poorer aerodynamic performance.

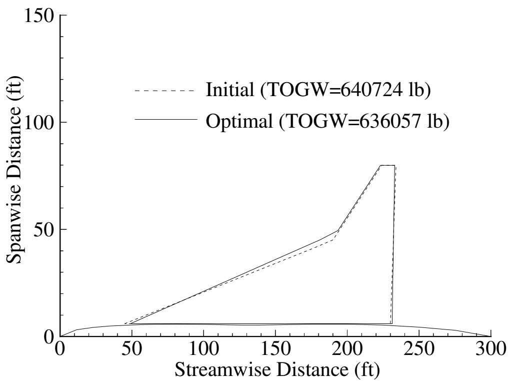

Figure 10. Five variable initial and optimal designs obtained without using RS models.

6.4 Computational Expense

The computational expense of performing a complete five variable HSCT wing optimization using the RS models is approximately 0.75 CPU minutes on a Silicon Graphs Indigo^2 workstation. In comparison, an optimization without using the RS models requires approximately 30 CPU minutes. As described above, the computational expense of the VCRSM method occurs in the creation of the RS models. For the five variable problem the cost of creating the RS models is approximately four CPU hours. Thus, optimization performed using the VCRSM method has a lower computational cost than traditional optimization for this HSCT design problem if more than eight traditional optimizations are performed. In a typical study the HSCT design optimization is performed many more than eight times. For example, the designer will perform the HSCT optimization starting with several different choices for the initial variable values. In addition, the designer often repeats the optimization to explore different objective criteria (e.g., maximize range, maximize payload). Therefore, the computational expense of creating the RS models is quickly recovered in a typical HSCT optimization study.

7. HSCT Wing Design Problem - Ten Variables

7.1 Conceptual Level HSCT Analyses

A 3^{10} full factorial design (i.e., three levels in each variable) was constructed around an initial HSCT configuration. The 59,049 (3^{10}) full factorial design points were analyzed using the inexpensive, conceptual level analysis tools and the HSCT analysis results were screened to eliminate from consideration any grossly infeasible HSCT configurations. Here an HSCT configuration was eliminated if it violated any of the geometric constraints by more than five percent. After screening 29,163 HSCT configurations remained; 51 percent of the original HSCT candidate configurations were eliminated.

7.2 Preliminary Level HSCT Analyses

The next step in the VCRSM process was to select a set of 132 D-optimal HSCT configurations from the remaining candidate set of 29,163. For this problem, an in-house version of Mitchell's k-exchange algorithm was used to create the D-optimal experimental design. The distribution of the 132 D-optimal HSCT configurations within the design space gives a condition number of 27 for the matrix $\mathbf{X}$, which allows the estimation of the RS model terms without significant numerical error.

The 132 D-optimal HSCT configurations were evaluated using the preliminary level analysis methods. Quadratic RS models, each having 66 coefficients, were created for C_{Dwave}, $C_{L\alpha}$ at M=2.4, ${C_T/C_L}^2$, and $C_{L\alpha}$ at M=0.2. The $R^2{}_{adj}$ values for these RS models were 0.9603, 0.9976, 0.9982, and 0.9979, respectively. Regression analyses were performed on these RS models and coefficients that did not have a t-statistic greater than 6.31 were removed. The recomputed $R^2{}_{adj}$ values for the RS models were 0.9667, 0.9978, 0.9986, and 0.9983, respectively. All of the recomputed $R^2{}_{adj}$ values were only slightly greater, so the original RS models with all 66 coefficients were retained for use.

The results of the regression analyses indicated that the C_{Dwave} RS model was most strongly influenced by 17 coefficients. These included all of the linear terms except for $C_{tip}, b_{nacelle}$, and W_{fuel}, and included the quadratic terms for $t/c\ ratio$ and Λ_{LE_I}. The 31 coefficients in the $C_{L\alpha}$ (M=2.4) RS model included all of the linear terms except for $max.\ thk.$, and included the quadratic terms for $C_{root}, b_{half}, R_{LE}\ param., t/c\ ratio$, and Λ_{LE_I}. The 17 coefficients in the ${C_T/C_L}^2$ RS model contained the linear terms for $C_{root}, C_{tip}, b_{half}$, $R_{LE}\ param.$, Λ_{LE_I}, and Λ_{LE_O}, along with the quadratic terms for C_{root}, Λ_{LE_I}, and Λ_{LE_O}. The 18 coefficients in the $C_{L\alpha}$ (M=0.2) RS model included the linear terms for $C_{root}, C_{tip}, b_{half}, t/c\ ratio, \Lambda_{LE_I}$, and Λ_{LE_O}, along with the quadratic terms for C_{root}, b_{half}, and Λ_{LE_I}. In summary, all of the linear coefficients are important in at least one of the RS models and six of the quadratic coefficients ($C_{root}, t/c\ ratio, b_{half}$, $R_{LE}\ param., \Lambda_{LE_I}$, Λ_{LE_O}) are important in at least one of the RS models.

The average error, RMS error, and maximum error for the complete RS models (66 coefficients) are shown in Table 6, where the residual error calculations are performed for the data from the 132 HSCT analyses used to create the RS models. Note that the residual errors are considerably higher for C_{Dwave} and ${C_T/C_L}^2$ in the ten variable RS models than in the five variable RS models.

Table 6. Accuracy of the response surface models for the ten variable HSCT optimization.

	Avg. Error	**RMS Error**	**Max. Error**
C_{Dwave}	4.36%	5.78%	18.31%
$C_{L\alpha}$ at M=2.4	0.21%	0.27%	0.91%
${C_T/C_L}^2$	8.39%	13.19%	47.45%
$C_{L\alpha}$ at M=0.2	0.24%	0.30%	0.90%

For C_{Dwave} the increase in residual error is the result of bias error since the magnitude of the numerical noise in the C_{Dwave}, data is known to be small compared to typical values of C_{Dwave} (see Section 3.1). In contrast, for ${C_T/C_L}^2$ the increase in residual error is due to numerical noise error. It is known that the leading edge thrust estimation methods are extremely sensitive to changes in the HSCT planform. This sensitivity produces numerical noise in the ${C_T/C_L}^2$ data where the magnitude of the noise may be up to 25 percent of typical ${C_T/C_L}^2$ values[36]. Although a predicted value for ${C_T/C_L}^2$ from the RS model may contain significant error, the supersonic drag-due-to-lift calculation is dominated by the $C_{L\alpha}$ (M=2.4) term. Thus, there is minimal effect on the overall HSCT wing design due to the residual error in the ${C_T/C_L}^2$ RS model. Also, note that for the initial HSCT configuration the range computed using the RS models is 5,503.7 *naut.mi.* and the range computed using the original methods is 5,519.8 *naut.mi.*, a difference of 0.29 percent.

7.3 HSCT Optimization - Ten Variables

Using the RS models, various initial HSCT configurations were optimized, within the allowable limits of the ten variables. Figure 11 shows the planform changes from the initial to the optimal wing configuration for one of these optimization cases. The initial and optimal wing variables are listed in Table 7. The optimal wing has a smaller area and a lower aspect ratio than the initial wing which results in a wing structural weight savings of 23,500 *lb*, a decrease of 18.3 percent. In addition to the structural improvements, the $(L/D)_{max}$ of the HSCT increased from 9.37 to 9.54, an improvement of 1.8 percent. This contributes to a savings in fuel weight of approximately 18,000 *lb*. The initial and optimal wing configurations are also shown in an isometric view in Figure 12 where the difference in the chordwise location of maximum thickness is more apparent. Additional optimization cases were performed, each with a different set of initial wing variables. In all cases, the optimizer converged to wing configurations virtually identical to the optimal wing described above.

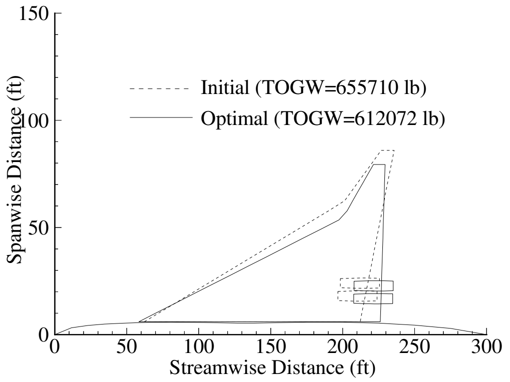

Figure 11. Ten variable initial and optimal wing designs obtained using RS models.

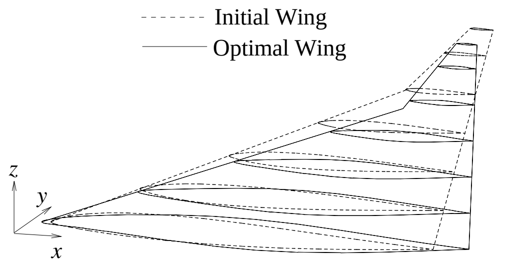

Note: The x-z plane is scaled to show airfoil differences.

Figure 12. Ten variable initial and optimal wing designs (with RS models) showing airfoil differences.

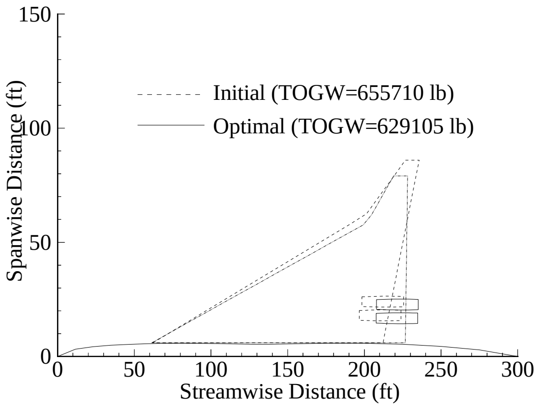

Figure 13. Ten variable initial and optimal wing designs obtained without using RS models.

For the optimal HSCT wing configuration, the range computed using the RS models is 5,500.2 *naut.mi.* whereas the range computed using the original methods is 5,393.2 *naut.mi.*, a difference of 1.98 percent. Since the true range is below 5,500 *naut.mi.*, the HSCT configuration would need to carry additional fuel to meet the range constraint. This would add approximately 9,600 *lb* to the TOGW of the HSCT, an increase of 1.57 percent in TOGW for the optimal HSCT configuration.

When optimization was attempted without using the RS models, the various initial wing configurations converged to substantially different optimal configurations. This is consistent with the occurrence of multiple local optima and the convergence difficulties which originally motivated the use of RS modeling methods. One such locally optimal design is shown in Figure 13. The HSCT with the locally optimal wing design in Figure 13 is 17,000 *lb* heavier than the HSCT with the globally optimal wing design.

Table 7. Ten HSCT wing initial and optimal variables.

Variable	**Initial**	**Optimal**
C_{root}	150.0 ft	167.7 ft
C_{tip}	9.0 ft	8.1 ft
$t/c\ ratio$	2.1 %	2.3 %
b_{half}	80.0 ft	73.4 ft
$max.\ thk.$	33.0 %	47.5 %
$R_{LE}\ param.$	2.5	2.1
Λ_{LE_I}	68.0°	71.1°
Λ_{LE_O}	47.0°	40.3°
$b_{nacelle}$	18.0 ft	16.7 ft
W_{fuel}	319,000 lb	300,700 lb

7.4 Computational Expense

The computational expense of performing a complete ten variable HSCT wing optimization using the RS models is approximately 1.5 CPU minutes on a Silicon Graphs Indigo^2 workstation. In comparison, an optimization without using the RS models requires approximately 60 CPU minutes. The computational cost of creating the RS models is approximately 55 CPU hours when the HSCT analyses are performed serially. However, if the parallel computing methods of Burgee[25] et al. were applied to this problem, it is estimated that the computational cost would be reduced to approximately five CPU hours. It is apparent that the computational affordability of the VCRSM method depends on the extent to which parallel computing may be used to reduce the computational cost of creating the RS models. Without parallel computing there is little or no computational savings in using the VCRSM method. Conversely, with parallel computing the computational savings in using the VCRSM method quickly accrue.

8. Conclusions

Response surface modeling methods have been combined with statistical techniques from design of experiments theory to create *variable complexity response surface modeling.* The results of this study show that the use of the VCRSM method avoids the convergence difficulties encountered in numerical optimization due to numerical noise. In this particular investigation, the VCRSM method was used to design optimal wing configurations for an HSCT aircraft, subject to aerodynamic and structural constraints. Both five variable and ten variable wing design problems were studied.

The aerodynamic analysis methods used in this HSCT optimization study produced numerical noise which would misdirect or slow the convergence of the optimization process if not addressed. The VCRSM method was used to select a limited number of HSCT configurations for analysis. From the resulting analysis data, response surface models were created to approximate four computationally expensive aerodynamic quantities. These were the supersonic volumetric wave drag C_{Dwave}, the supersonic lift curve slope $C_{L\alpha}$ at M=2.4, the supersonic leading edge thrust $C_T/{C_L}^2$, and the subsonic lift curve slope $C_{L\alpha}$ at M=0.2. The response surface models were then used to perform the five and ten variable HSCT wing design optimizations.

In the five variable HSCT wing optimization problem the use of the response surface models allowed the identification of the globally optimal wing configuration. which had a TOGW which was 14,000 *lb* less than for the artificial, locally optimal wing configuration found without using the response surface models. This represents a savings of 2.1 percent in TOGW. The five variable optimization problem was repeated for several cases, each starting with a different initial wing configuration. When using the response surface models, each case converged to the globally optimal wing configuration. In contrast, without using the RS models, each case converged to a locally optimal wing configuration significantly heavier than the global optimum.

Similar results were obtained in the ten variable HSCT wing optimization problem where the globally optimal wing configuration identified using the response surface models was 17,000 *lb* lighter than the corresponding artificial, locally optimal wing configuration. This yielded a savings of 2.7 percent in TOGW. Several optimization cases were conducted for the ten variable optimization problem, each starting with a different initial wing configuration. Again, in all cases where the response surface models were employed the globally optimal wing configuration was consistently identified by the optimizer. Without using the response surface models, the optimizer became trapped in the artificial, locally optimal wing configurations created by the presence of numerical noise.

Acknowledgments

This research was supported by NASA Grant NAG-1-1562 with Dr. Perry Newman as the contract monitor.

References

1. Giunta, A. A., Dudley, J. M., Narducci, R., Grossman, B., Haftka, R. T., Mason, W. H., and Watson, L. T., "Noisy Aerodynamic Response and Smooth Approximations in HSCT Design," *Proceedings of the 5th AIAA/USAF/NASA/ISSMO Symposium on Multidisciplinary Analysis and Optimization,* Panama City Beach, FL, Sept. 1994, pp. 1117–1128.
2. Dudley, J., Huang, X., MacMillin, P. E., Grossman, B., Haftka, R. T., and Mason, W. H., "Multidisciplinary Optimization of the High-Speed Civil Transport," AIAA Paper 95–0124, Reno, NV, Jan. 1995.
3. Gill, P. E., Murray, W., and Wright, M. H., *Practical Optimization,* Academic Press, Inc., San Diego, CA, 1981.
4. Nelder, J. A., and Mead, R., "A Simplex Method for Function Minimization," *Comput. J.,* Vol. 7, 1965, pp. 308–313.
5. Jayaram, S., Myklebust, A., and Gelhausen, P., "ACSYNT – A Standards-Based System for Parametric Computer Aided Conceptual Design of Aircraft," AIAA Paper 92–1268, Feb. 1992.
6. McCullers, L. A., "Aircraft Configuration Optimization Including Optimized Flight Profiles," *Proceedings of the Symposium on Recent Experiences in Multidisciplinary Analysis and Optimization,* Sobieski, J. (ed.), NASA CP-2327, April 1984, pp. 396–412.
7. Frank, P. D., Booker, A. J., Caudell, T. P., and Healy, M. J., "A Comparison of Optimization and Search Methods for Multidisciplinary Design," *Proceedings of the 4th AIAA/USAF/NASA/OAI Symposium on Multidisciplinary Analysis and Optimization,* Cleveland, OH, Sept. 1992, pp. 1040–1057.
8. Sobieszczanski-Sobieski, J., Haftka, R. T., "Multidisciplinary Aerospace Design Optimization: Survey of Recent Developments," AIAA 96–0711, Reno, NV, Jan. 1996.
9. Montgomery, D. C., *Design and Analysis of Experiments,* John Wiley & Sons, New York, NY, 1976, pp. 180–263, 340–364.
10. Myers, R. H., and Montgomery, D. C., *Response Surface Methodology: Process and Product Optimization Using Designed Experiments,* John Wiley & Sons, New York, NY, 1995, pp. 1–15, 22, 297–305, 363–370.
11. Healy, M. J., Kowalik, J. S, and Ramsay, J. W., "Airplane Engine Selection by Optimization on Surface Fit Approximations," *J. Aircraft,* Vol. 12, No. 7, 1975, pp. 593–599.
12. Craig, J. A., Jr., "D-Optimal Design Method: Final Report and User's Manual," General Dynamics

Report FZM-6777 for Air Force Contract F33615-78-C-3011, June 1978.

13. Engelund, W. C., Stanley, D. O., Lepsch, R. A., McMillin, M. M., and Unal, R., "Aerodynamic Configuration Design Using Response Surface Methodology Analysis," AIAA Paper 93–3967, Monterey, CA, Aug. 1993.
14. Giunta, A. A., Narducci, R., Burgee, S., Grossman, B., Mason, W. H., Watson, L. T., and Haftka, R. T., "Variable-Complexity Response Surface Aerodynamic Design of an HSCT Wing," *Proceedings of the 13th AIAA Applied Aerodynamics Conference,* San Diego, CA, June 1995, pp. 994–1002.
15. Tai, J. C., Mavris, D. N., and Schrage, D. P., "Application of a Response Surface Method to the Design of Tipjet Driven Stopped Rotor/Wing Concepts," AIAA Paper 95-3965, Los Angeles, CA, Sept. 1995.
16. Sellar, R. S., Stelmack, M. A., Batill, S. M., and Renaud, J. E., "Response Surface Approximations for Discipline Coordination in Multidisciplinary Design Optimization," AIAA Paper 96–1383, Salt Lake City, UT, April 1996.
17. Davis, P. "Industrial-Strength Optimization At Boeing," *SIAM News,* Vol. 29, No. 1, January/February 1996.
18. Yesilyurt, S., Ghaddar, C. K., Cruz, M. E., Patera, A. T., "Bayesian-Validated Surrogates for Noisy Computer Simulations; Application to Random Media," (to appear) *SIAM J. Sci. Comp.,* Vol. 17, No. 4, July 1996.
19. Kroo, I., Altus, S., Braun, R., Gage, P., and Sobieski, I., "Multidisciplinary Optimization Methods for Aircraft Preliminary Design," *Proceedings of the 5th AIAA/USAF/NASA/ISSMO Symposium on Multidisciplinary Analysis and Optimization,* Panama City Beach, FL, Sept. 1994, pp. 697–707.
20. Gilmore, P., and Kelley, C. T., "An Implicit Filtering Algorithm for Optimization of Functions with Many Local Minima," *SIAM J. Opt.,* Vol. 5, No. 2, May 1995. pp. 269–285.
21. Gage, P., and Kroo, I., "A Role for Genetic Algorithms in a Preliminary Design Environment," AIAA Paper 93–3933, Monterey, CA, Aug. 1993.
22. Aly, S., Marconi, F., Ogot, M., Pelz, R., and Siclari, M., "Stochastic Optimization Applied to CFD Shape Design," *Proceedings of the 12th AIAA Computational Fluid Dynamics Conference,* San Diego, CA, June 1995, pp. 11–20.
23. Siclari, M. J., Van Nostrand, W., Austin, F., "The Design of Transonic Airfoil Sections for an Adaptive Wing Concept Using a Stochastic Optimization Method," AIAA Paper 96–0329, Reno, NV, Jan. 1996.
24. Torczon, V., "On the Convergence of Pattern Search Algorithms," (to appear) *SIAM J. Opt.,* 1996.
25. Burgee, S., Giunta, A. A., Balabanov, V., Grossman, B., Mason, W. H., Narducci, R., Haftka, R. T., and Watson, L. T., "A Coarse Grained Parallel Variable-Complexity Multidisciplinary Optimization Paradigm," (to appear) *Intl. J. Supercomputing Applications and High Performance Computing,* 1996.
26. *DOT Users Manual, Version 4.20,* Vanderplaats Research & Development, Inc., Colorado Springs, CO, 1995.
27. Knill, D. L., Balabanov, V., Grossman, B., Mason, W. H., and Haftka, R. T., "Certification of a CFD Code for High-Speed Civil Transport Design Optimization," AIAA Paper 96–0330, Reno, NV, Jan. 1996.
28. Carlson, H. W., and Walkley, K. B., "Numerical Methods and a Computer Program for Subsonic and Supersonic Design and Analysis of Wings with Attainable Thrust Considerations," NASA CP 3808, 1984.
29. Harris, R. V., Jr., "An Analysis and Correlation of Aircraft Wave Drag," NASA TM X-947, 1964.
30. *GENESIS Users Manual, Version 1.3,* Vanderplaats, Miura and Associates, Inc., Goleta, CA, 1993.
31. Kaufman, M., Balabanov, V., Burgee, S., Giunta, A. A., Grossman, B., Mason, W. H., Watson, L. T., and Haftka, R. T., "Variable-Complexity Response Surface Approximations for Wing Structural Weight in HSCT Design," AIAA Paper 96-0089, Reno, NV, Jan. 1996.
32. Narducci, R., Grossman, B., Valorani, M., Dadone, A., and Haftka, R. T., "Optimization Methods for Non-smooth or Noisy Objective Functions in Fluid Design Problems," *Proceedings of the AIAA 12th Computational Fluid Dynamics Conference,* June 1995, pp. 21–32.
33. Box, M. J. and Draper, N. R., "Factorial Designs, the $|\mathbf{X}^T\mathbf{X}|$ Criterion, and Some Related Matters," *Technometrics,* Vol. 13, No. 4, 1971, pp. 731–742.
34. *JMP Users Guide, Version 3.1,* SAS Institute, Inc., Cary, NC, 1995.
35. Mitchell, T. J., "An Algorithm for the Construction of D-Optimal Experimental Designs," *Technometrics,* Vol. 16, No. 2, May 1974, pp. 203-210.
36. Hutchison, M. G., "Multidisciplinary Optimization of High-Speed Civil Transport Configurations Using Variable-Complexity Modeling," Ph.D. Dissertation, VPI&SU, March 1993.

Appendix

Table A-1. Twenty-nine HSCT variables and nominal values.

Num.	Value	Description
1	181.48	Wing root chord, ft
2	155.9	LE break point, x ft
3	49.2	LE break point, y ft
4	181.6	TE break point, x ft
5	64.2	TE break point, y ft
6	169.5	LE wing tip, x ft
7	7.00	Wing tip chord, ft
8	75.9	Wing semi-span, ft
9	0.40	Chordwise max. thk. location
10	3.69	LE radius parameter
11	2.58	Airfoil t/c *ratio* at root, %
12	2.16	Airfoil t/c *ratio* at LE break, %
13	1.80	Airfoil t/c *ratio* at tip, %
14	2.20	Fuselage restraint 1, x ft
15	1.06	Fuselage restraint 1, r ft
16	12.20	Fuselage restraint 2, x ft
17	3.50	Fuselage restraint 2, r ft
18	132.46	Fuselage restraint 3, x ft
19	5.34	Fuselage restraint 3, r ft
20	248.67	Fuselage restraint 4, x ft
21	4.67	Fuselage restraint 4, r ft
22	26.23	Nacelle 1 location, ft
23	32.39	Nacelle 2 location, ft
24	697.9	Vertical tail area, ft^2
25	713.0	Horizontal tail area, ft^2
26	39,000	Thrust per engine, lb
27	322,617	Mission fuel, lb
28	64,794	Starting cruise/climb altitude, ft
29	33.90	Supersonic cruise/climb rate, ft/min

Table A-2. Constraints for the 29 variable HSCT optimization problem.

Num.	Geometric Constraints
1	Fuel volume $\leq$ 50% wing volume
2	Airfoil section spacing at $C_{tip} \geq 3.0ft$
3-20	Wing chord $\geq 7.0ft$
21	LE break $\leq$ semi-span
22	TE break $\leq$ semi-span
23	Root chord t/c *ratio* $\geq$ 1.5%
24	LE break chord t/c *ratio* $\geq$ 1.5%
25	Tip chord t/c *ratio* $\geq$ 1.5%
26-30	Fuselage restraints
31	Nacelle 1 outboard of fuselage
32	Nacelle 1 inboard of nacelle 2
33	Nacelle 2 inboard of semi-span
Num.	**Aero. & Performance Constraints**
34	Range $\geq 5,500$ *naut.mi.*
35	C_L at landing ≤ 1
36-53	Section C_l at landing ≤ 2
54	Landing angle of attack $\leq 12°$
55-58	Engine scrape at landing
59	Wing tip scrape at landing
60	LE break scrape at landing
61	Rudder deflection $\leq 22.5°$
62	Bank angle at landing $\leq 5°$
63	Tail deflection at approach $\leq 22.5°$
64	Takeoff rotation to occur $\leq V_{min}$
65	Engine-out limit with vertical tail
66	Balanced field length $\leq$ 11,000 ft
67-69	Mission segments: thrust available$\geq$ thrust required

Table A-3. Constraints for the five variable HSCT wing optimization problem.

Num.	Geometric Constraints
1	Fuel volume $\leq$ 50% wing volume
2	Airfoil section spacing at $C_{tip} \geq 3.0ft$
3-20	Wing chord $\geq 7.0ft$
21	LE break $\leq$ semi-span
22	Airfoil t/c *ratio* $\geq$ 1.5%
Num.	**Aero. & Performance Constraints**
23	Range $\geq 5,500$ *naut.mi.*
24	C_L at landing ≤ 1
25-42	Section C_l at landing ≤ 2